Volume 20, No 4 | International Journal of Radiation Research, October 2022

Study on the factors affecting the dose error of using I-125 seeds in the treatment of prostate cancer using the Monte Carlo method

H. Gao[1,2], Y. Wang[1,2], C. Du[1,2], X. Li[1,2], K. Liu[1,2], H. Xue[1,2], W. Tang[1,2], L. Chen[1,2], C. Yan[1,2], Y. Tu[1,2], L. Sun[1,2*]

[1]State Key Laboratory of Radiation Medicine and Protection, School of Radiation Medicine and Protection, Soochow University, Suzhou 215123, China
[2]Collaborative Innovation Centre of Radiation Medicine of Jiangsu Higher Education Institutions, Suzhou 215123, China

► ***Original article***

Corresponding author:
Liang Sun, Ph.D.,
E-mail:
slhmz666@suda.edu.cn

Received: August 2021
Final revised: April 2022
Accepted: May 2022

Int. J. Radiat. Res., October 2022; 20(4): 857-864

DOI: 10.52547/ijrr.20.4.19

Keywords: *radioactive seed implantation, interseed attenuation effect, Monte Carlo, I-125 seed source.*

ABSTRACT

***Background*:** NatuAt present, radioactive seed implantation is a common treatment for prostate cancer, the TPS (treatment planning system) calculates the dose by adding the dose attributed to each source. However, the interseed attenuation effect would result in a difference between the actual dose and the calculated dose. The aim of this study was to identify the factors influencing the interseed attenuation effect. ***Materials and Methods*:** I-125 seed sources were selected, and MC (Monte Carlo) method was used to simulate the dose distribution around seed sources. The results obtained from the linear addition of a single-source dose were compared with those obtained considering the interseed attenuation effect. The effects of the medium, source arrangement and source number on the dose were evaluated. ***Results*:** The MC simulation results for multiple seed sources are lower than those for linear additive doses in most areas. In different medium, the mean error caused by interseed attenuation effect is the smallest in adipose tissue (0.52%) and the largest in bone (1.41%). Taking four sources as examples, the maximum error is 9.34%, appearing in the plane where the source is located. The error decreases to 1.3% when the source is located 2 mm away from the source plane. The more scattered the sources are in space, the smaller the error will be. ***Conclusions*:** A high atomic number and high-density medium will cause a high error. The area with a high error is mainly observed in the plane where the sources are located, the edge error of the source distribution area is larger.

INTRODUCTION

Prostate cancer is a common primary tumor in men worldwide. More than a quarter of a million men die of prostate cancer every year [1]. Since Pasteau first used I-125 for prostate implantation [2], the application of I-125 seeds in the treatment of prostate cancer has become increasingly common. At present, brachytherapy is one of the most common treatment options for prostate cancer [3-5]. Because of its advantage of little effect on surrounding tissues and organs and short recovery period, it exerts good therapeutic effects on untreated primary tumors, important functional tissues that need to be retained, and locally advanced tumors. An increasing number of patients with prostate cancer are expected to receive this treatment in the future [6, 7].

I-125 is a commonly used radionuclide for treatment, with a half-life of 59.4 days, and it is produced by the decay of γ photons with an average photon energy of 28.37 keV. The radioactive material is sealed with biocompatible material. During treatment, the treatment planning system (TPS) is used to select the number and locations of seed source implantation sites, and the radioactive seed are implanted into the anterior column gland under the guidance of transrectal ultrasound. Based on the premise of ensuring the target volume dose coverage, the minimal dose is administered to reduce potential damage to other organs [8].

At present, most of the dose calculations obtained using the treatment planning system are based on the line source calculation model recommended by AAPM TG-43U1 [9, 10], which simply adds the dose attributed to each source administered to the position of interest. However, the actual seed sources will influence each other, resulting in a deviation between the actual dose and the calculated dose. This difference is caused by the interseed attenuation effect [11, 12] and tissue heterogeneity [13, 14]. The interseed attenuation effect is defined as a lower actual deposited energy than the calculated value due to the mutual blocking between seed sources, mainly resulting from substances with a high atomic number,

[DOI: 10.52547/ijrr.20.4.19]

such as silver and titanium, constituting the seed source. Tissue heterogeneity refers to the phenomenon of calculation error caused by the effect of the main components and scattering components of the radiation field in an uneven medium [15].

The dose distribution after seed source implantation is very important. As a dose-result related treatment method Accurate calculation of the dose distribution is the basis and key to the success of the treatment scheme, the dose distribution after implantation directly determines the efficacy and the severity of complications. Therefore, it is of great clinical significance to consider the attenuation of the seed source [16].

Some studies have discussed the effects of various factors on the dose of the seed source, Ali proposed that the interseed attenuation effect will reduce the dose by an average of 6% [17, 18]; Amal *et al.* found that the titanium structure of the seed source will attenuate the energy by 19% [19]; Burns *et al.* [11] simulated the attenuation of the I-125 seed source in water and determined that the perturbation effect should not be ignored and may cause the isodose curve to bend inward. Mason *et al.* [20] measured the attenuation of the I-125 seed source in prostate brachytherapy and compared the error when the seed source diameter was 0.8 and 0.5 mm, and the dose was reduced by as much as 18%. When few seed sources were used, the reduction was small. Chibani *et al.* [21] studied the dosimetric effects of anisotropy and intermediate attenuation of Pd103 and I-125 sources in prostate implantation and compared the Monte Carlo method, isotropic point source dose-kernel superposition (PSKS) and line source dose-kernel superposition (LSKS); In the case of four seed sources, PSKS overestimated the dose by 4% - 6% and LSKs overestimated the dose by 2% - 5%. The effect of different media on the error has also been studied. Carrier *et al.* [22] discussed the effects of the number of seed sources and local heterogeneity on the error in the case of two prostate sizes. Tamura *et al.* [23] used PHITS to discuss the effects of interspecific attenuation and tissue composition on the dose distribution in the prostate. Mobit *et al.* [12] studied the attenuation of 27 uniformly distributed seed sources in water, compared the errors of seed source spacings of 1.00 cm, 0.75 cm and 0.50 cm, and considered that the disturbance error decreased with increasing seed source spacing but did not further explore different arrangement methods. Recently, some studies have also focused on the optimization of clinical algorithms. Safigholiden *et al.* [24] proposed a new calculation formula based on artificial intelligence to modify the dose that considers the interaction between seeds; Mountris [25] developed a Monte Carlo dose optimization algorithm based on dose volume histograms.

At present, the effect of the arrangement of seed sources on the calculation error is rarely discussed, and studies of the optimization of the dose calculation method are also very limited and cannot be used in the clinic. The innovation of this study is to quantitatively analyze the error caused by the difference between the interseed attenuation effect of the seed source and different media, analyze the effect of different factors on the error, and provide the layout of the seed source to reduce the error. Based on the aforementioned studies, the commonly used radioactive I-125 source [26-28] was selected as the research object in this study, and the Monte Carlo software MCNP5 was used to further evaluate the factors influencing the interseed attenuation effect of the source to determine the error size of the source in different media and the relationship between the source arrangement, number and dose perturbation. The dose attenuation results of each layer in the case of multilayer seed distribution are provided to quantitatively analyze the error caused by the interseed attenuation effect of the seed source and more accurately calculate the dose of the seed source. This paper systematically evaluates the interference effect of seed source distribution and provides a reference from the perspective of reducing the error for evaluating the dose distribution of clinical seed source implantation radiotherapy.

MATERIALS AND METHODS

I-125 seed source

I-125 seed source (Model 6711) is a commonly used clinical radiation source [19, 29-31]. The model used in this paper is derived the literature [32]. It is used as a simulation object. The overall length is 4.5 mm, and the appearance is cylindrical. The internal silver wire is a small cylinder with a length of 3.25 mm and a diameter of 0.5 mm, and I-125 is placed on the cylindrical surface of the silver wire. The cladding is titanium, the thickness at both ends of the source is 0.5 mm, and the thickness around the source is 0.05 mm. The model is shown in figure 1(A). The energy and yield of the I-125 source used in the calculation are derived from a previous study [33], and details are shown in table 1.

Monte Carlo software

The Monte Carlo method has been widely used to analyze the dosimetric characteristics of brachytherapy seed sources [34-37]. MCNP5 (Monte Carlo N-particle transport5) [38] is a Monte Carlo radiation transport program developed by Los Alamos National Laboratory that has been proven to be able to accurately simulate the dose distribution of seed source brachytherapy [9, 20, 39, 40]. This study uses MCNP5 software for the simulation.

Calculation method

Simulate the dose distribution of seed source in the medium. The dose of I-125 decreases rapidly within 1 cm [41], and the effect on the results of the

[DOI: 10.52547/ijrr.20.4.19]

dose calculation at distances greater than 2 cm can be ignored [42]. Therefore, the dose calculation range is set to a cube of 6 cm×6 cm×6 cm, the seed source is located in the center of the cube. The proportions of material elements used in the simulation are derived from the ICRP44 report [43, 44]. In the set dose calculation range, * Fmesh card was divided into 1 mm×1 mm×1 mm grid points, the photon energy fluence at the center of each grid point was calculated, and then 'DEn/DFn' card was used to multiply the mass energy absorption coefficient to convert it into dose [45].

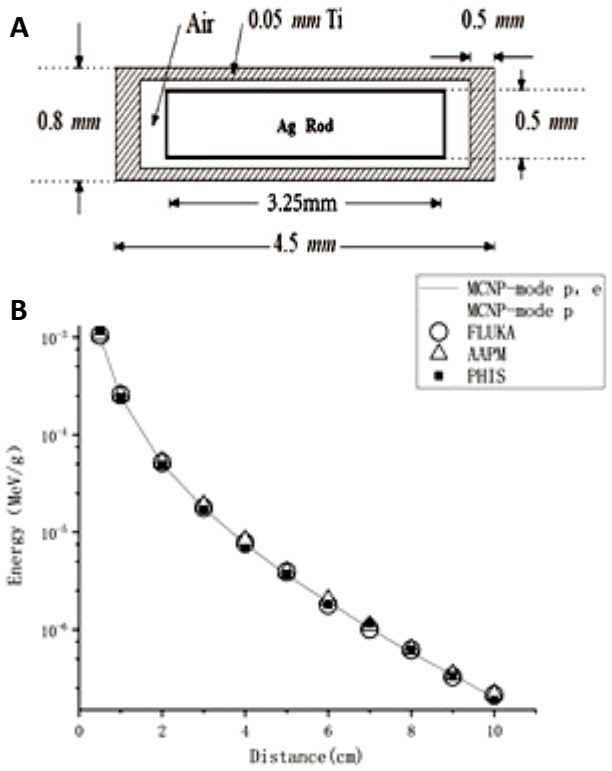

Figure 1. Schematic diagram of I-125 seeds, Model 6711 **(A)** and a comparison of the vertical dose obtained using different methods for calculating the seed source **(B)**.

Table 1. I-125 source energy and yield.

Energy(MeV)	0.0272	0.0275	0.0310	0.0317	0.0355
Probability	0.406	0.757	0.202	0.044	0.067

After verification, we determined that the decision of whether to track electrons had little effect on the calculation results. The results are shown in figure 1-B, but the calculation time was substantially reduced. Therefore, the 'mode P' option was used to turn off electronic tracking and increase computational efficiency [21], the calculated particle number was set to 2×10^9, and the calculation error was less than 5%. This approach reaches the credibility level of the MCNP calculation [46]. The computing platform used in the present study is produced by the China Inspur company. The operating system is a quad core 2.3 GHz Intel (R) Xeon (R) E5-2696 CPU with 256 GB of Samsung-DDR4 memory.

Method for comparing perturbation error

First, the dose distribution of a single seed at different position sources was measured using MCNP5 and recorded as k_1, k_2 … k_i, and its linear superposition value $\sum k_i$ was defined as the total dose without considering the interseed attenuation effect. Then, the dose distribution of all seed sources was calculated by performing a Monte Carlo simulation ,and the inhomogeneity and interseed attenuation effect caused by other seed sources were clearly considered and could be regarded as the actual dose value [47] , defined as K.

The ratio of K and $\sum k_i$ is defined as D and is shown in equation (2):

$$D=\frac{K}{\sum k_i} \quad (2)$$

The ratio of K and $\sum k_i$ is defined as D and is shown in equation (2):

$$D=\frac{K}{\sum k_i} \quad (2)$$

D is the degree of interaction between seed sources. The closer the value is to 1, the smaller the error. If the value is larger than 1, the linear superposition result is lower than the actual value (Monte Carlo simulation value). If the value is smaller than 1, the linear superposition result is higher than the actual value.

At the same time, F is defined as the absolute error, which is calculated using equation (3):

$$F = |1 - D| \quad (3)$$

The average error, MSE (mean-square error) and median error of F are used as evaluation indices, and MSE is defined using equation (4):

$$MSE = \frac{\sum_{n=1}^{n} F(n)^2}{n} \quad (4)$$

Where n is the number of counted points.

This paper focuses on the interseed attenuation effect caused by I-125 sources, and thus no specific dose is provided, and only the error is shown.

Model verification

In order to verify the correctness of the model, different modes of MCNP5 mode P(do not electronic tracking), mode P E (electronic tracking), and different Monte Carlo software FLUKA [48] and PHITS [49] are used to simulate the dose of 0.5, 1, 2, 3, 4, 5, 6, 7, 8, 9, 10 cm at the center line of the seed source. The calculation results of line source equation (5) proposed by AAPM- TG43U [9-10] are compared, and the results are shown in figure 1(B), ensuring the correctness of the simulation.

$$D(r,\theta) = S_k \cdot \Lambda \cdot \frac{G_{L(r,\theta)}}{G_L(r_0\theta_0)} \cdot g_L(r) \cdot F(r,\theta) \quad (5)$$

G_L is the geometric function, g_L is the radial dose

[DOI: 10.52547/ijrr.20.4.19]

function, and F is the anisotropic function. R and Θ represent the distance between the point of interest and the center of the seed source in polar coordinates and the angle between the line of the point of interest and the center of the seed source and the long axis direction of the seed source, respectively. r_0, Θ_0, represents the position 1 cm away from the vertical axis of the seed source with an angle of 90 degrees. S_k is the air kerma intensity, and Λ is the dose rate per unit air kerma at the reference point of liquid water.

Simulation of the influencing factors of media types

This study first calculated the dose value of a single seed source in different media, compared it with the equivalent medium water used by TG43, and calculated the relative error to compare the effects of different media on the calculation error.

Then, two parallel seed sources with a distance of 1 cm were established. The arrangement is shown in figure 2(A); one is placed at the (- 0.5, 0, 0) point, and the other is placed at the (0.5, 0, 0) point, calculating the absolute error F for each counting point caused by interseed attenuation effect in different media.

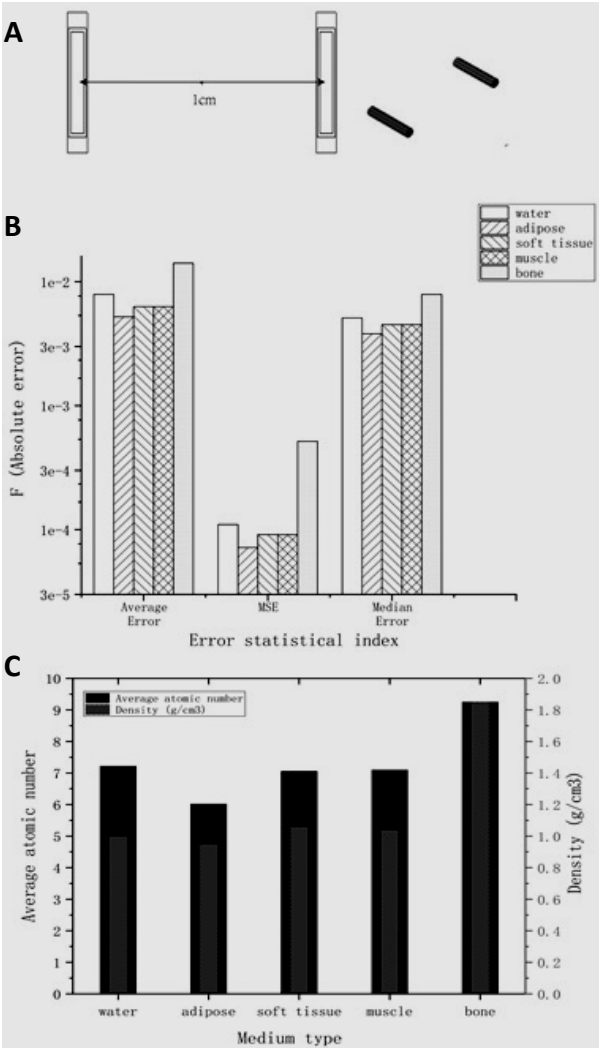

Figure 2. Source distribution diagram **(A)**, absolute error F for soft tissue, fat, muscle, water and bone **(B)** and their average atomic numbers and density **(C)**.

Simulation of the influence factors of the arrangement and the number of sources

The effects of 16 different arrangements of 2-21 sources, the same vertical axis, the same straight line and multilayer distribution on the dose perturbation error were compared. The distance between adjacent sources was 1 cm, and the medium was water.

8. Comparison with the clinical source distribution.

In clinical treatment, the number of seed sources actually used generally ranges from 30 to 100 according to the actual condition [20,50], but if all seed sources are considered, the value exceeds the range of seed source interactions and increases the calculation time. Therefore, this paper only focuses on the seed sources in the range of interaction and provides an example of the arrangement of seed sources used in the clinic, according to the literature [42,50]. Ten seed sources were set in the area of interest and arranged in three layers: three seed sources in the top layer, four in the middle layer and three in the lower layer, with a spacing of 1 cm. The specific arrangement mode is shown in figure 3 (A) and compared with the arrangement mode used in this study.

RESULTS

Source error in different media

As shown in the present study, the average errors of counting points of bone, muscle, soft tissue and fat were 88.55%, 3.52%, 4.62% and 11.42%, respectively, compared with water. Figure 2(B) shows the statistical chart of the dose error F of the seed source in different media. Figure 2(C) shows the average atomic numbers and densities of those media. The error of muscle and soft tissue is very close, and the error in bone is the largest (1.41%), the smallest error is observed in adipose tissue (0.52%), and increases in relative atomic mass and density gradually increase the error.

Results of simulations using different arrangements

This study takes four sources and twenty-one sources as examples, the square arrangement in the same plane, the upper and lower arrangement, the same long axis arrangement , the same vertical axis arrangement and 21 sources randomly distributed in space / evenly distributed in the center are simulated. The influence of different source distribution on the error is analyzed. Fig. 4(A) shows the 3D spatial distribution of D values. Because the source is symmetrically distributed, 1/8 of the data (coordinates x<0, y<0, z>0) is removed to show its internal distribution. Figure 4(B) shows the error histograms of different arrangement modes.

[DOI: 10.52547/ijrr.20.4.19]

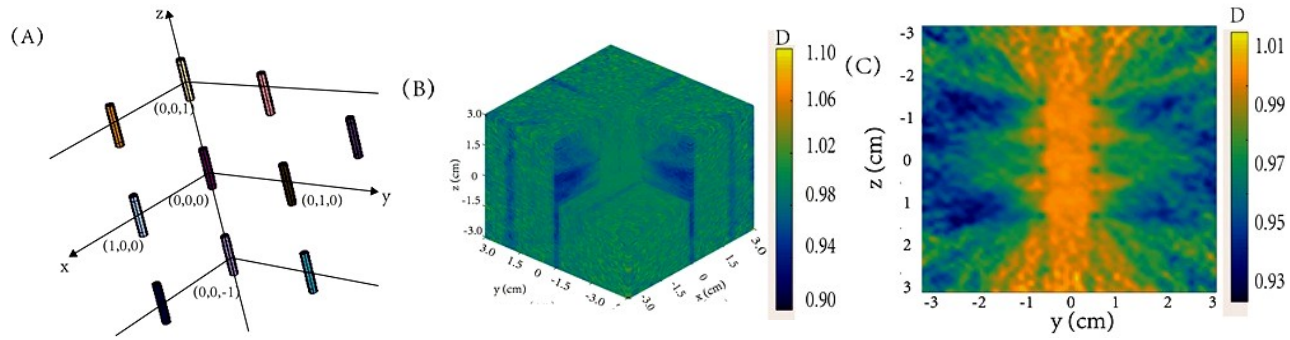

Figure 3. Source source distribution mode **(A)**, three-dimensional error **(B)** of the clinical source and x = 0 plane error **(C)** of the clinical.

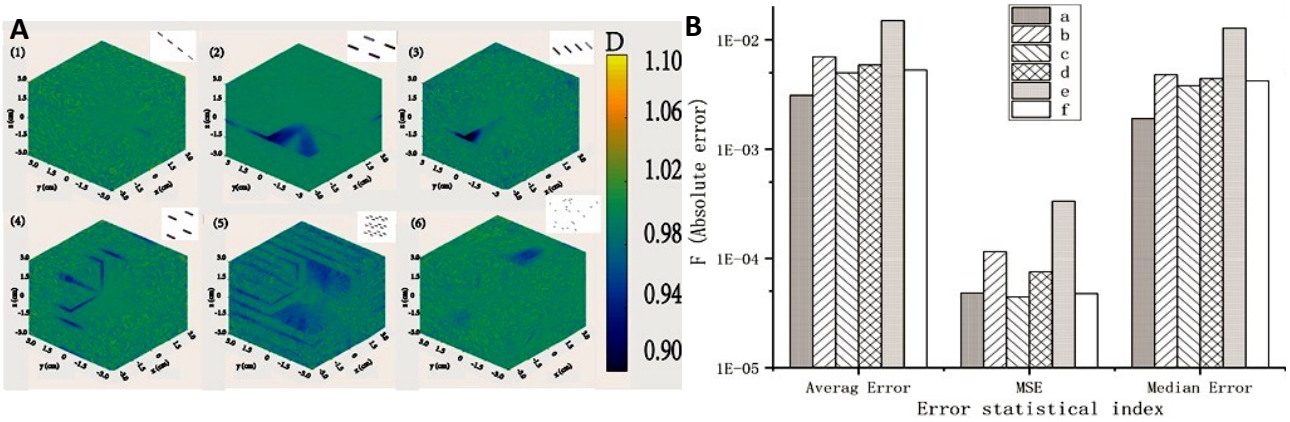

Figure 4. Comparison of different arrangements of 4 sources, 21 sources regularly arranged in an random order **(A)**; 4 sources arranged in a square on the same plane **(a)**, arranged in two layers **(b)**, arranged in the same long axis **(c)**, arranged in the same vertical axis **(d)**, and evenly arranged in the center **(e)**; and 21 sources randomly distributed in space **(f)** error histogram **(B)**.

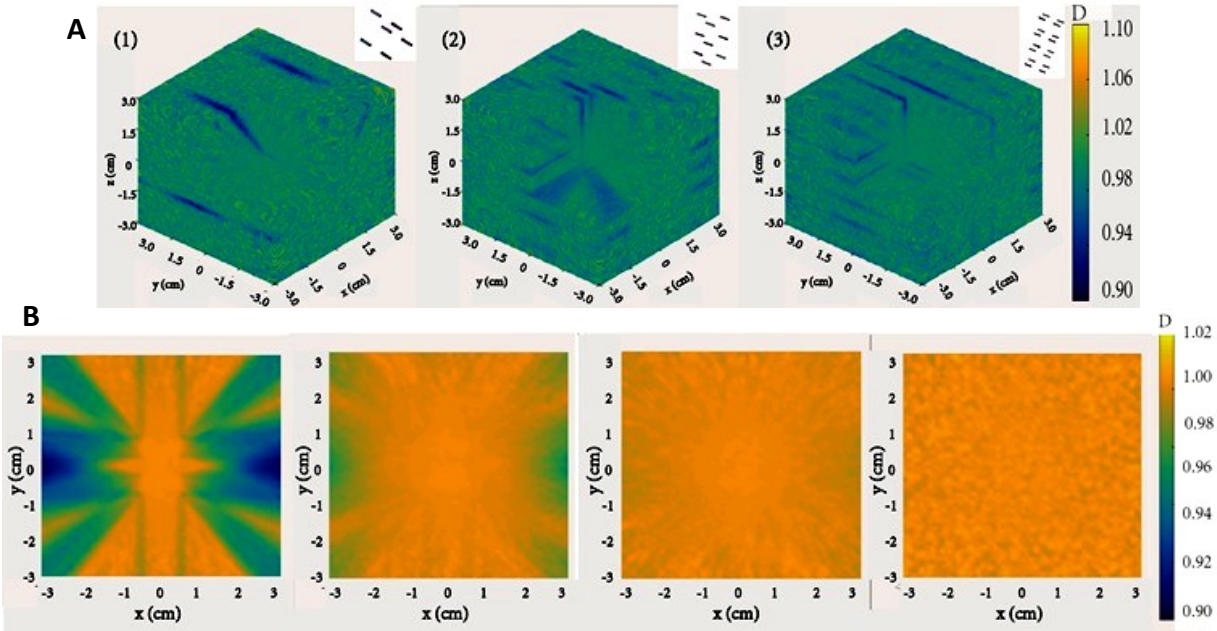

Figure 5. Error diagrams for 6, 9, and 16 sources with a multilayer arrangement **(A)** and the error diagram for 4 sources in the Z = 0, 1, 2, and 30 mm plane **(B)**.

High error distribution area

Figure 5(A) shows the error diagrams for 6, 9, and 16 sources with a multilayer arrangement. As shown in figure 5(A), the error attributed to the interseed attenuation effect is only larger in the plane where the source is located. Figure 5(B) shows the uniform arrangement of four sources in the same plane as an example and provides the results obtained for seeds located 0, 1, 2, and 30 mm away from the plane of the source. The error caused by the interaction of sources is very small when the source is 1 mm away from the plane where the source is located. The maximum error is 4.1%, and almost no error is observed when the source is 2 mm away, the

[DOI: 10.52547/ijrr.20.4.19]

maximum error is only 1.3%. By comparing the distribution of multiple sources in the same plane with the error 3D distribution map, the error is mainly concentrated in the edge area, and the error in the internal area is small.

The effect of the number of different sources on the error

To eliminate the effect of different source distributions on the error ,the source distribution must remain unchanged when increasing the number of sources . The error distribution of 2-6 sources in the same vertical axis and the error distribution with 3, 4, 6 and 9 sources in the same plane are compared. Figures 6 (A, B) show the error histograms for 3, 4, 6 and 9 sources in the same plane and 2, 3, 4, 5, and 6 sources in the same vertical axis. Figures 6 (D, F) show the 3D spatial distributions of D values, figure 6 (C, E) show the distributions of D values in the z=0 plane.

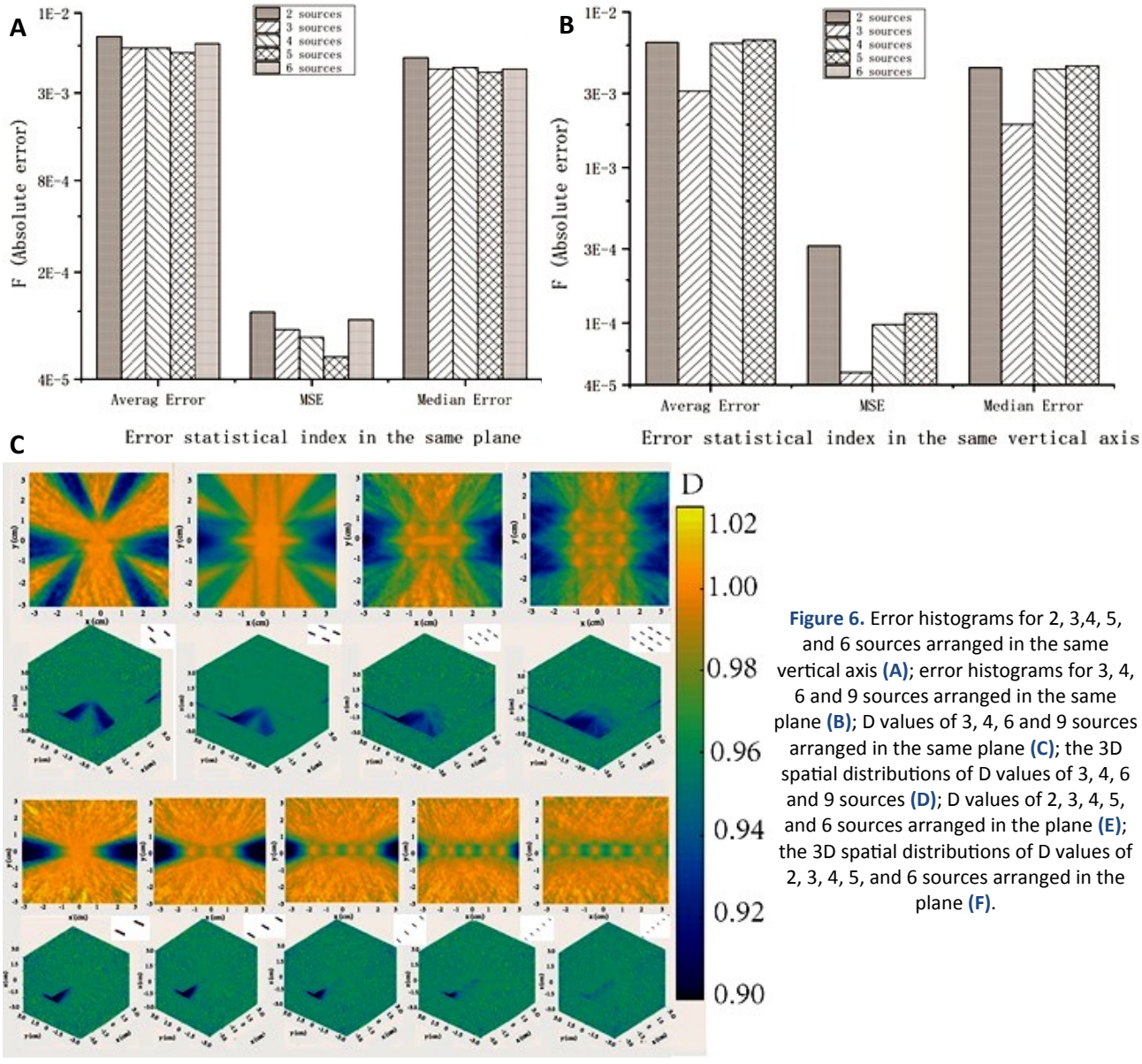

Figure 6. Error histograms for 2, 3,4, 5, and 6 sources arranged in the same vertical axis **(A)**; error histograms for 3, 4, 6 and 9 sources arranged in the same plane **(B)**; D values of 3, 4, 6 and 9 sources arranged in the same plane **(C)**; the 3D spatial distributions of D values of 3, 4, 6 and 9 sources **(D)**; D values of 2, 3, 4, 5, and 6 sources arranged in the plane **(E)**; the 3D spatial distributions of D values of 2, 3, 4, 5, and 6 sources arranged in the plane **(F)**.

Error of clinical source distribution mode

The error caused by the clinical source distribution is shown in figure 3. Figure 3(B) shows the three-dimensional spatial distribution of the D value, and figure 3(C) shows the distribution of the D value in the x=0 plane, the maximum error reaches 13.17%.

DISCUSSION

Serhat believed that the dose difference of I-125 source in prostate tissue and aqueous medium ranged from 7.2% to 10.5% [51]. Considering the content of various tissues of prostate, it was basically consistent with the conclusion of this paper. It can be

[DOI: 10.52547/ijrr.20.4.19]

seen that there is a large gap between bon the water medium used by TG43, which is one of the main sources of error. Moreover, the obvious interseed attenuation effect of bone may explain the findings reported by Haidari *et al.* [52] that calcification in the prostate will cause dose cold spots.

Figures 2(B) and 2(C) show that the error distribution is closely related to the position of the source. The smallest values are obtained for the three error indices when the sources are evenly arranged in the same vertical axis, the largest values are obtained when they are arranged in the same line. The more scattered the same number of sources are in space, the smaller the error caused by their mutual disturbance, and the maximum error reaches 12.7%， Mobit *et al.* [12] proposed that no difference existed in the dose volume histogram between a simple superposition model and complete Monte Carlo simulation when the source spacing was 1 cm, but we thought the error should not be ignored; and the error is very similar to the measurement results reported by Meigooni and others using thermo luminescent dosimetry (TLD). They found that the error between the results of the TPS and TLD is approximately 10% [17]. Stephen *et al.* studied Pd-103 sources and found that compared with the seeds aligned with the implant angle, the average difference of the vertically arranged seed sources in skin dose was 4% [53]. In this study, the average difference of two arrangement modes in I-125 seed source is 5.64%, which indicates that I-125 seed is more affected by angle.

And when the arrangement mode is the same, with the increase of the number of sources, the error is not that Carrier *et al.* [22] think that the perturbation error will increase with the increase of the number of seed sources, but will gradually stabilize. It is speculated that the first reason is that the source doses at different positions complement each other, weakening the attenuation effect caused by the blocking between different sources. Secondly, the reflection effect of the source metal shell to make up for the dose loss; Finally, as mentioned above, the high error region is mainly in the region far from the source, which exceeds the region of interest.

According to previous studies [17, 21-24], most of the results obtained are higher than the actual value (Monte Carlo calculation value) based on the linear addition, but the dose of linear addition is also lower in some areas. There are two main reasons for the conjecture. One is the effect of the reflection of the outer shell of the seed source, because the reflection of the material with high atomic number of the source shell is not considered in the linear superposition. The second is the inherent error of Monte Carlo calculation.

At the same time, from figures 3(B, C) , the error of clinical source distribution mode is biger than uniform source distribution mode, it has much room for improvement by considering the error caused by the interseed attenuation effect. The future research direction is to ensure that this value is as close to the real dose as possible by implementing various correction factors.

CONCLUSIONS

We use the Monte Carlo method to calculate the error caused by the mutual disturbance of sources in different cases. The number, arrangement and medium type of sources affect the error,. The effect of source interaction on the unified plane is large, and the effect of different levels is very small. The error between sources is small, and the error in the edge area is large. We hope that the aforementioned conclusions will provide guidance for clinical source distribution, reduce the calculation error of the region of interest and ensure a more accurate dose distribution.

ACKNOWLEDGEMENTS

None.

***Conflicts of interest*:** Declared none.

***Funding*:** This study was supported by Jiangsu Higher Education Institutions; China funding of the National Natural Science Foundation of China, China (Grant No. 12105200); China funding of the National Natural Science Foundation of China, China(Grant No. 12175161); the Priority Academic Program Development of Jiangsu Higher Education Institutions (PAPD) China; and the Nuclear Energy Development Project, China (No. 2016- 1295), the National Natural Science Foundation of China (grant numbers U186720).

***Author contribution*:** HG and YG wrote the manuscript. YW assisted the data collection and performed analyses data. LS designed the research, and developed the direction of the manuscript. CD, XL, KL reviewed the writing of each section. HX, WT, LC, CY, YT puts forward some guidance for the idea of the article. All authors contributed to the manuscript preparation and discussions.

REFERENCES

1. Juste B, Miró R, Morató S, *et al.*(2020) Prostate cancer Monte Carlo dose model with 177Lutetium and 125Iodine treatments. *Radiat Phys Chem, **174**: 108908*.
2. Machtens S, Baumann R, Hagemann J, *et al.* (2006) Long-term results of interstitial brachytherapy (LDR-Brachytherapy) in the treatment of patients with prostate cancer. *World J Urol, **24**: 289-295*.
3. Holm HH, Juul N, Pedersen JF, *et al.* (2002) Transperineal 125iodine seed implantation in prostatic cancer guided by transrectal ultrasonography. *J Urology, **167**: 985-988*.
4. Holm H and Gammelgaard J (1981) Ultrasonically guided precise needle placement in the prostate and the seminal vesicles. *J Urology, **125**: 385-387*.
5. Skowronek J (2017) Current status of brachytherapy in cancer treatment–short overview. *J Contemp Brachyther, **9**: 581*.
6. Tanaka N, Fujimoto K, Hirao Y, *et al.* (2009) Variations in international prostate symptom scores, uroflowmetric parameters, and

[DOI: 10.52547/ijrr.20.4.19]

prostate volume after 125I permanent brachytherapy for localized prostate cancer. *Urology, **74**: 407-411*.
7. Jinming H and Ningwen Y (2020) Progress of permanent seed implantation using 125I-seeds for cancer therapy. *J Isotopes, **33**: 186*.
8. Carrier J-F, D'Amours M, Verhaegen F, *et al.* (2007). Postimplant dosimetry using a Monte Carlo dose calculation engine: a new clinical standard. *Int J radiat Oncol, **68**: 1190-1198*.
9. Rivard MJ, Coursey BM, DeWerd LA, Hanson WF, *et al.* (2003) Update of the AAPM task group no. 43 report - a revised AAPM protocol for brachytherapy dose calculations. *Int J Radiat Oncol Biol Phys, **57**: S430*.
10. Rivard MJ, Coursey BM, Dewerd LA, *et al.* (2004) Update of AAPM Task Group No. 43 Report: A revised AAPM protocol for brachytherapy dose calculations. *Med Phys, **31**: 633-674*.
11. Burns GS and Raeside DE (1989) The accuracy of single-seed dose superposition for I-125 implants. *Med Phys, **16**: 627-631*.
12. Mobit P and Badragan I (2004) Dose perturbation effects in prostate seed implant brachytherapy with I-125. *Phys Med Biol, **49**: 3171-3178*.
13. Meigooni Ali S (1992) Tissue inhomogeneity correction for brachytherapy sources in a heterogeneous phantom with cylindrical symmetry. *Med Phys, **19**: 401-407*.
14. Kirov AS, Williamson JF, Meigooni AS, *et al.* (1996) Measurement and calculation of heterogeneity correction factors for an Ir-192 high dose-rate brachytherapy source behind tungsten alloy and steel shields. *Med Phys, **23**: 911-919.*
15. Miksys N, Haidari M, Vigneault E, *et al.* (2017) Coupling I-125 permanent implant prostate brachytherapy Monte Carlo dose calculations with radiobiological models. *Med Phys, **44**: 4329-4340*.
16. Stock RG, Stone NN, Tabert A, *et al.* (1998) A dose–response study for I-125 prostate implants. *Int J Radiat Oncol, **41**: 101-108*.
17. Meigooni AS, Meli JA, Nath R (1992) Interseed effects on dose for 125I brachytherapy implants. *Med Phys, **19**: 385-390*.
18. Afsharpour H, D'Amours M, Coté B, *et al.* (2008) A Monte Carlo study on the effect of seed design on the interseed attenuation in permanent prostate implants. *Med Phys, **35**: 3671-3681*.
19. Yasiri AYA, Abed HF (2018) Estimation of Energy Spectrum and Energy Deposition of Photons Emitted from Brachytherapy 125 I Seed. *Indian J Sci Tec, **11**: 1-5*.
20. Mason J, Al-Qaisieh B, Bownes P, *et al.* (2013) Monte Carlo investigation of I-125 interseed attenuation for standard and thinner seeds in prostate brachytherapy with phantom validation using a MOSFET. *Med Phys, **40**: 031717*.
21. Chibani O, Williamson JF, Todor D (2005) Dosimetric effects of seed anisotropy and interseed attenuation for 103Pd and 125I prostate implants. *Med Phys, **32**: 2557-2566*.
22. Carrier JF, Beaulieu L, Therriault-Proulx F, *et al.*(2006) Impact of interseed attenuation and tissue composition for permanent prostate implants. *Med Phys, **33**: 595-604*.
23. Tamura K, Araki F, Ohno T (2016) SU-F-T-46: The Effect of Inter-Seed Attenuation and Tissue Composition in Prostate 125I Brachytherapy Dose Calculations. *Med Phys, **43**: 3471-3472*.
24.Safigholi H, Sardari D, Jashni SK, *et al.* (2013) An analytical model to determine interseed attenuation effect in low-dose-rate brachytherapy. *J Appl Clin Med Phys, **14**: 4226*.
25. Mountris KA, Visvikis D, Bert J (2019) DVH-based inverse planning using Monte Carlo dosimetry for LDR prostate brachytherapy. *Int J Radiat Oncol, **103**: 503-510*.
26. Al-Qaisieh B, Bownes P, Roberts G (2012) Evaluation of the visibility of a new thinner 125I radioactive source for permanent prostate brachytherapy. *Brachytherapy, **11**: 460-467*.
27. Johnson M, Colonias A, Parda D, *et al.* (2006) Dosimetric and technical aspects of intraoperative I-125 brachytherapy for stage I non -small cell lung cancer. *Med Phys, **33**: 2089-2090*.
28. Wallner K, Merrick G, True L, *et al.* (2002) I-125 versus Pd-103 for low-risk prostate cancer: morbidity outcomes from a prospective randomized multicenter trial. *Cancer Journal, **8**: 67-73*.
29. Rivard MJ (2009) A dosimetric comparison of the model 6711 125I source and a new, smaller diameter brachytherapy seed (model 9011) using Monte Carlo methods. *Brachytherapy, **8**: Issu 2*.
30. Kenichi T, Tsuyoshi K, Takahiro H, *et al.* (2018) An *in-vitro* verification of strength estimation for moving an 125I source during implantation in brachytherapy. J Radiat Res, **59**(4): 484-489.
31. Rivard MJ (2009) Monte Carlo radiation dose simulations and dosimetric comparison of the model 6711 and 9011 125I brachytherapy sources. *Med Phys, **36**: 486-491*.
32. Williams J (1997) The interdependence of staff and patient doses in interventional radiology. *Brit J Radiol, **70**: 498-503*.
33.Seltzer SM, Lamperti PJ, Loevinger R, *et al.* (2003) New National Air-Kerma-Strength Standards For 125I and 103Pd Brachytherapy Seeds. *J Res Natl Inst Stand Technol, **108**: 337-358*.
34.Williamson and Jeffrey F (1988) Monte Carlo evaluation of specific dose constants in water for 125I seeds. *Med Phys, **15**: 686-694*.
35. Wang R and Li XA (2000) A Monte Carlo calculation of dosimetric parameters of 90Sr/90Y and 192Ir SS sources for intravascular brachytherapy. *Med Phys, **27**: 2528-2535*.
36. Wierzbicki JG, Rivard MJ, Waid DS, *et al.*(1998). Calculated dosimetric parameters of the IoGold 125I source model 3631-A. *Med Phys, **25**: 2197-2199*.
37. Chibani O and Li XA (2003) IVBTMC, A Monte Carlo dose calculation tool for intravascular brachytherapy. *Med Phys, **30**.*
38. Team X-MC. MCNP-Version 5, Vol. I: Overview and Theory. 2003.
39. Rivard MJ (2001) Monte Carlo calculations of AAPM Task Group Report No. 43 dosimetry parameters for the MED3631-A/M125I source. *Med Phys, **28**: 629*.
40. Chibani O and Li XA (2002) Monte Carlo dose calculations in homogeneous media and at interfaces: a comparison between GEPTS, EGSnrc, MCNP, and measurements. *Med Phys, **29**: 835–847*.
41. He J, Zhang H, Wang J, *et al.* (2012) Study on distribution of 125 I seed source dose field. *Rad Prot Bulletin, **32**: 36-38*.
42. Li Z, Jiang S, Yang Z, *et al.* (2015) Monte Carlo simulation and experimental investigation of 125 I interseed dose attenuation. *Chinese J RAD MEDI and PROT, **35**: 389-392*.
43. Kurudirek M (2014) Effective atomic numbers and electron densities of some human tissues and dosimetric materials for mean energies of various radiation sources relevant to radiotherapy and medical applications. *Radiat Phys Chem, **102**: 139-146*.
44. Goldstone K (1989) Tissue substitutes in radiation dosimetry and measurement, in: ICRU Report 44, International Commission on Radiation Units and Measurements, USA. WB Saunders; 1990.
45. Hubbell JH and Seltzer SM (1995) Tables of X-ray mass attenuation coefficients and mass energy-absorption coefficients 1 keV to 20 MeV for elements Z= 1 to 92 and 48 additional substances of dosimetric interest. National Inst. of Standards and Technology-PL.
46. Reed AL (2007) Medical physics calculations with MCNP: a primer. Boston, MA: Los Alamos National Laboratory, X-3 MCC, LA-UR-07-4133.
47. Duggan DM (2004) Improved radial dose function estimation using current version MCNP Monte-Carlo simulation: Model 6711 and ISC3500 125I brachytherapy sources. *Appl Radiat Isot, **61**:1443-1450*.
48. Fasso A, Ferrari A, Ranft J, *et al.* (2005) FLUKA: a multi-particle transport code. CERN-2005-10.
49. Niita K, Sato T, Iwase H, *et al.* (2006) PHITS—a particle and heavy ion transport code system. *Radiat Meas, **41**: 1080-1090*.
50. Reis JP, Menezes AF, Souza EM, *et al.* (2012) Dose optimization in 125I permanent prostate seed implants using the Monte Carlo method. *Comput Phys Commun, **183**: 847-852*.
51. Serhat A (2021) The investigation of tissue composition effects on dose distributions using Monte Carlo method in permanent prostate brachytherapy. *Clin Exper Heal Sci, **11**: 769-774*.
52. Ali-Reza, Mehan, Haidari, *et al.* (2019) Dosimetric and radiobiological investigation of permanent implant prostate brachytherapy based on Monte Carlo calculations. *Brachytherapy, **18**: s 875-882*.
53. Deering SG, Hilts M, Batchelar D, *et al.* (2021) Dosimetric investigation of 103Pd permanent breast seed implant brachytherapy based on Monte Carlo calculations. *Brachytherapy, **20**: 686-694*.

[DOI: 10.52547/ijrr.20.4.19]